

<https://doi.org/10.1038/s43247-024-01712-0>

Temporal dynamics in vertical leaf angles can confound vegetation indices widely used in Earth observations

Check for updates

Teja Kattenborn ^{1,2,3} ✉, Sebastian Wieneke ^{2,3}, David Montero ^{2,3}, Miguel D. Mahecha ^{2,3,4}, Ronny Richter ^{3,5}, Claudia Guimarães-Steinicke ^{2,3}, Christian Wirth ^{3,5}, Olga Ferlian ^{3,6}, Hannes Feilhauer ^{2,3,4}, Lena Sachsenmaier ^{3,5}, Nico Eisenhauer ^{3,6} & Benjamin Dechant ^{3,7}

Earth observation data is key for monitoring vegetation dynamics across temporal and spatial scales. The most widely used method to estimate vegetation properties from Earth observation data is vegetation indices. However, temporal dynamics in vertical leaf angles can strongly alter reflectance signals and, hence, vegetation indices. Here, we derive leaf angles from plant photographs to simulate the effect on vegetation indices with radiative transfer models. We show that leaf angle dynamics systematically confound widely applied vegetation indices. Moreover, we demonstrate that these effects are not random but tightly linked to abiotic environmental conditions. These systematic effects of vertical leaf angles have implications for monitoring plant properties, biodiversity, and ecosystem functional properties. We discuss the related challenges and opportunities to assess spatio-temporal vegetation dynamics with remote sensing and vegetation indices.

Since the seventies, Earth observation satellites have been providing crucial data on vegetation dynamics in time and space¹. Optical satellite sensors are of particular value for monitoring terrestrial ecosystem dynamics, given that plant canopies have evolved to interact with light. The reflectance of plants across wavelengths can inform about various biophysical and -chemical properties. The fractions of light reflected at visible wavelengths, for instance, are indicative of pigment concentrations. Reflectances in the near and short-wave infrared regions are sensitive to biochemical and structural properties and components such as cellulose, water, and lignin^{2,3}. Hence, temporal changes in reflectance measured from satellites provide an extremely effective basis for monitoring such plant properties across ecosystems.

However, the reflectance at a particular wavelength cannot trivially be translated into plant properties, such as leaf pigment or water contents, because many plant properties determine radiative transfer processes in overlapping wavelengths through scattering and absorption. Therefore, the estimation of plant properties from reflectance signals is commonly based on a combination of multiple wavelengths. The most widely used empirical approach uses vegetation indices (VIs) as proxies, combining two or more spectral bands of different wavelengths^{4,5}. VIs enable the estimation of

specific vegetation properties by reducing or suppressing background signals or confounding factors related to vegetation characteristics with overlapping spectral features. More than 130 indices have been proposed to *indicate* different plant properties⁶. These have been applied in a plethora of vegetation-related studies, ranging from monitoring plant vitality⁷, assessing global greening and browning^{8,9}, inferring functional diversity^{1,10}, estimating biophysical state variables, such as leaf area index (LAI), the fraction of absorbed photosynthetically active radiation (FAPAR) or above-ground biomass^{11,12}, and deriving modes of climate variability^{13,14}. Many VIs can be derived across optical satellite missions, such as the MODIS and Landsat Missions (NASA) or the Sentinel-Missions (Copernicus, ESA)⁶ and are often available in the form of harmonized and ready-to-use products^{15,16}.

Although VIs are amongst the most frequently used tools for Earth observation data analytics, in terms of their interpretability, they often remain a black box because the vast biochemical and structural diversity of plants makes it difficult to precisely infer specific plant properties from reflectance spectra or derived indices^{1,17,18}. Especially the configuration of canopy structure and density is known to determine plant reflectance across visible to the shortwave infrared (400–2500 nm), by controlling light interception probabilities and scattering processes^{19–22}. The most important

¹Sensor-based Geoinformatics (geosense), Faculty for Environment and Natural Resources, University of Freiburg, Freiburg, Germany. ²Institute for Earth System Science and Remote Sensing, Leipzig University, Leipzig, Germany. ³German Centre for Integrative Biodiversity Research (iDiv) Halle-Jena-Leipzig, Leipzig, Germany. ⁴Helmholtz Centre for Environmental Research, Leipzig, Germany. ⁵Systematic Botany and Functional Biodiversity, Institute of Biology, Leipzig University, Leipzig, Germany. ⁶Experimental Interaction Ecology, Institute of Biology, Leipzig University, Leipzig, Germany. ⁷Leipzig University, Leipzig, Germany.

✉ e-mail: teja.kattenborn@geosense.uni-freiburg.de

canopy structural properties that affect light interception probabilities are (i) the total leaf surface area in a given area interacting with light (typically approximated by LAI), (ii) how these leaf surfaces are spatially clumped, and (iii) the vertical inclination of these leaf surfaces (Fig. 1), commonly described as leaf angle distributions.

While plant canopies are often perceived as stationary structures that typically develop over multiple years, already Charles Darwin acknowledged *The Power of Movement in Plants* and described short-term temporal changes in vertical surface angles of leaves²³. These leaf movements are driven by environmental conditions and can force an overall increase or decrease in vertical leaf angles^{24,25}. A prominent example are flaccid leaves that emerge from a loss of turgor pressure during drought or heat extremes²⁶. In such situations of leaf drooping, leaf surfaces typically tend to traverse from a horizontal (0°) or oblique to a more vertical orientation (90°).

Changes in vertical leaf surface angles induced by environmental dynamics may confound reflectance signals and, hence, VIs: On the one hand, vertical leaf angle dynamics may induce perturbing dynamics to vegetation index values. For example, an apparent leaf angle-induced change of a chlorophyll index value could be falsely interpreted as an actual change in chlorophyll content. On the other hand, the actual variation of a plant property might not be detectable due to the dominant influence of vertical leaf angle variation on reflectance. This may be crucial since strong vertical leaf angle dynamics may coincide with changes in other plant properties, e.g., during plant stress (Fig. 2, see also refs. 7,27).

So far, the confounding effect of vertical leaf angle dynamics on VIs is only marginally analyzed and acknowledged in the literature. Previous

studies attempted to assess these effects using radiative transfer models (RTMs)^{1,21,28–33}. These process-based models mimic the transfer of light from the sun through the plant canopies to the sensors as a function of biochemical and structural plant properties, including the leaf angle distribution (LAD) within a canopy. RTMs enable a specific assessment of the strong spectral imprint of LADs while controlling other factors that may affect reflectance signals, such as the variation in plant structural and biochemical traits, phenology, and soil background. However, the impact of LAD dynamics on vegetation reflectance remains an understudied phenomenon, since efficiently measuring LADs on long time scales at high temporal resolution was for a long time not feasible under field conditions^{34–36}. Therefore, previous studies were limited to using loosely defined LAD or sparse LAD observations of only one or very few plant species^{21,34}. Consequently, a clear understanding of the temporal coupling of LAD and VI dynamics is missing. Yet, recently, photographs from time-lapse cameras in concert with deep learning-based pattern recognition enable an effective tracking of LADs through time³⁷.

Here, we employ deep learning-derived LAD observations representative of typical satellite overpass times at solar noon as input for the radiative transfer model PROSAIL^{18,38} to expose the imprint of LAD dynamics on 124 established VIs (Fig. 3). During the year 2022 with meteorological and soil drought³⁹, LAD dynamics were recorded for 10 temperate deciduous tree species growing in dense, evenly-aged monocultures (MyDiv experiment, Germany)⁴⁰. Based on this analysis, we reveal that LAD dynamics can strongly confound many widely used VIs. In addition, we demonstrate that this effect varies with plant species and environmental conditions. This can result in systematic effects on VIs and their potential misinterpretation in remote sensing-based vegetation assessments, including plant biophysical state variables, vitality status, or functional diversity.

Results

All data were recorded in a growing season (day of year 158 to 279, 2022) when West-Central Europe was characterized by a substantial soil moisture drought and strongly elevated temperatures⁴¹. At our experimental site, the relative soil moisture (at 5, 10, and 55 cm depth) varied between 11.2 and 19.7% and fell below the wilting point of approximately 15% [estimated in ref. 42]. The temperature ranged between 7.8 and 27.8 °C, relative humidity between 48 to 85%, and vapor pressure deficit between 0.17 and 2.43 kPa. Along these strong environmental fluctuations (see Supplementary Fig. 1), vertical leaf angles varied substantially between the different tree species: The mean leaf angle at solar noon varied considerably for fast-growing species, such as *Prunus avium* (sd = 9.4°) and *Betula pendula* (sd = 8.5°) and

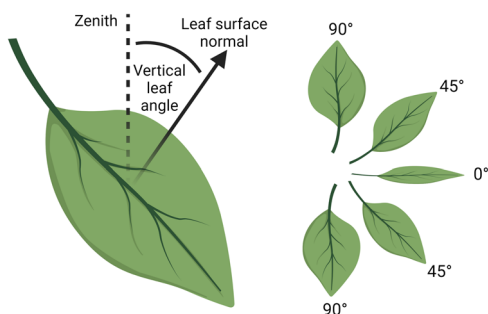


Fig. 1 | Definition of vertical leaf surface angles as the integrated angle of the entire leaf surface. A entirely horizontally oriented leaf corresponds to (0°) and a vertically oriented leaf to (90°).

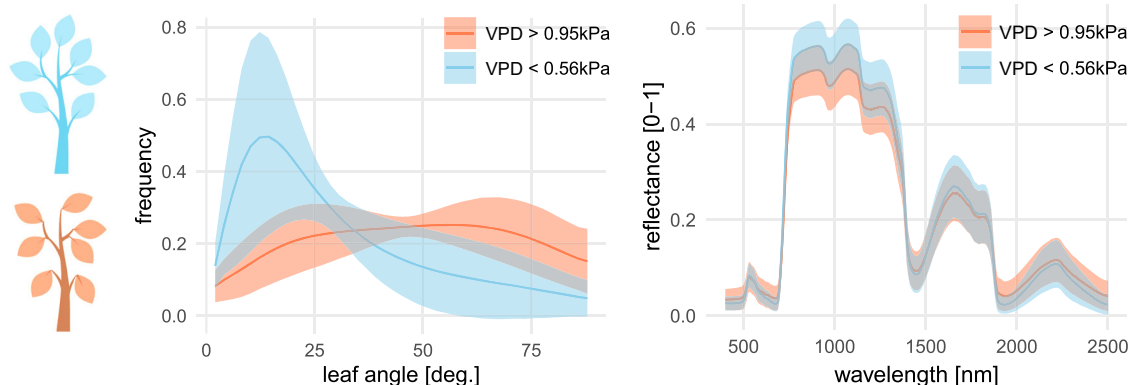


Fig. 2 | Environmental drivers, such as vapor pressure deficit (VPD), can modulate distributions of vertical leaf angles. Changes in leaf angle distributions (left) affect reflectance characteristics of plant canopies (right). The presented data is aggregated from daily leaf angle dynamics at the time of satellite overpass (solar noon) of *Prunus avium* tracked during a vegetation period in Bad Lauchstädt,

Germany. The reflectance data is simulated using radiative transfer models (see “Methods” section). Angles represent a horizontal (0°) and vertical orientation (90°). Note, that leaf angles (here defined as surface angle) typically increase when leaves are hanging.

Fig. 3 | Workflow of revealing the impact of vertical leaf angle dynamics on satellite-derived vegetation indices. The leaf angle observations are based on AngleCam³⁷, a computer vision method that was trained to derive leaf angle dynamics from plants in the foreground of plant photographs. For simplicity, the dynamics of vertical leaf angles are visualized as average leaf angles, while the Angle-Cam method³⁷ predicts leaf angle distributions between 0 to 90 degrees. The obtained leaf angle dynamics are then used as input to simulate the effect on 124 commonly used vegetation indices (VIs)⁶ through radiative transfer models.

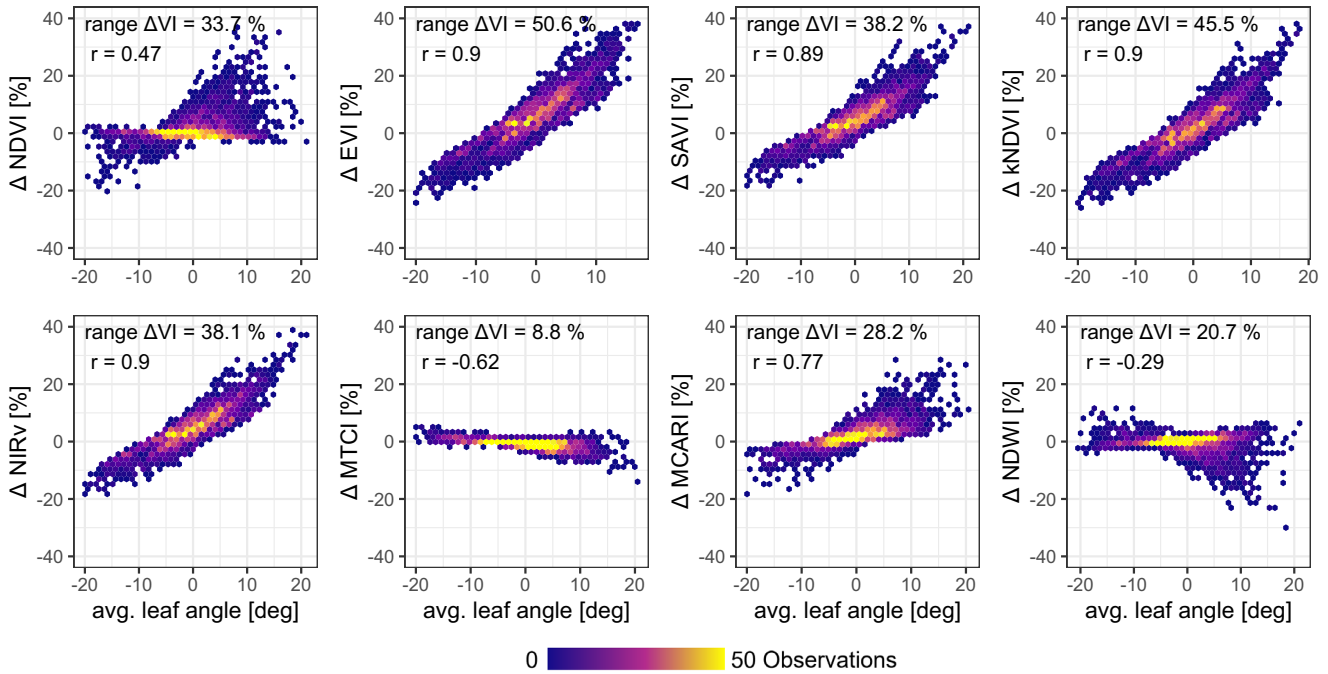
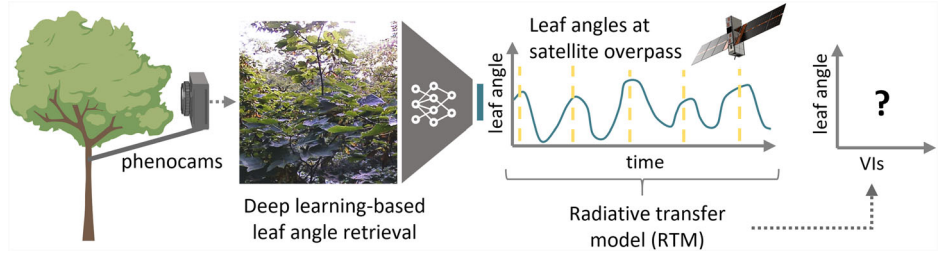


Fig. 4 | The effect ($\Delta VI\%$) of LAD dynamics on selected vegetation indices within the vegetation season. $\Delta VI\%$ was calculated as the relative difference between vegetation index values derived from simulated reflectance data with and without integrating actual vertical leaf angle dynamics. For visualization, LADs were

converted to average leaf angles. The VIs in the top row (NDVI, EVI, SAVI, kNDVI) are typically used for assessing the greenness of vegetation canopies, NIRv is used as proxy for the canopy structure, MTCI and MCARI for leaf chlorophyll content, while NDWI is a common proxy for leaf water content.

less for late successional species, such as *Quercus petraea* ($sd = 5.0^\circ$) and *Fraxinus excelsior* ($sd = 5.6^\circ$). Time series of daily leaf angle dynamics are shown in Supplementary Fig. 2.

For each LAD observation at satellite overpass times (here considered 10:00–11:00 am local solar time), we derived VIs from simulated canopy reflectance (PROSAIL radiative transfer model⁴³). Other vegetation properties relevant for radiative transfer simulations, including pigments, LAI, water, and dry matter content, were randomly sampled within ranges obtained from extensive data sources (for details see methods section)^{44,45}. The confounding effect of LADs on VIs (referred to as ΔVI) was determined as the difference of VIs derived from canopy reflectance simulated with (i) actual dynamics of LADs and (ii) average species-specific LADs. Since not all VIs share a similar dynamic range, we normalized ΔVI values by the obtained quantile range of each VI (onwards $\Delta VI\%$, Q_{01} and Q_{99}). For VIs frequently used for quantifying greenness (e.g. in the context of assessing vegetation vitality, density, or productivity), we observe a considerable range of $\Delta VI\%$: NDVI = 33.7%, SAVI = 38.2%, EVI = 50.5%, kNDVI = 45.3% (Fig. 4). Similar effects are found across all application types of VIs (Fig. 5a and Supplementary Fig. 3), including indices used for pigment assessments (e.g., MCARI, 28.23%) or leaf water content retrieval (e.g., NDWI =

20.68%). Thus, VIs differ in their sensitivity to LAD dynamics, affecting the specificity of a VI toward a designated target property (e.g., pigments).

Furthermore, we find that VIs differ strongly in their specificity to LAD dynamics, as quantified by the Pearson correlation coefficient (r , absolute values) ranging from 0 to 0.9 between the indices. Some indices, such as the NDVI, show a comparably moderate correlation to LAD dynamics ($r = 0.47$, Fig. 4). More sophisticated VIs that have been specifically designed to overcome saturation and structural effects observed in high-density plant canopies are exceptionally confounded by LAD dynamics ($r > 0.89$), including NIRv, SAVI, EVI, and kNDVI [for rationales on these VIs see refs. 46–49]. Note that other vegetation properties used as input for the reflectance simulation were by experimental design statistically independent from LAD dynamics. Thus, the partly high correlation of some VIs with LAD dynamics, such as for the pigment index MCARI ($r = 0.77$) or the greenness index kNDVI ($r = 0.89$), are not caused by actual changes in pigment contents or foliage density but by LAD dynamics alone.

Overall, we observe significantly higher $\Delta VI\%$ for VIs integrating spectral bands in the Near Infrared ($p < 0.01$) or Red bands ($p < 0.01$), while lower $\Delta VI\%$ are found for VIs integrating a shortwave infrared band (1610 nm, $p < 0.05$) or a Red-Edge band ($p < 0.02$). The correlation of VIs

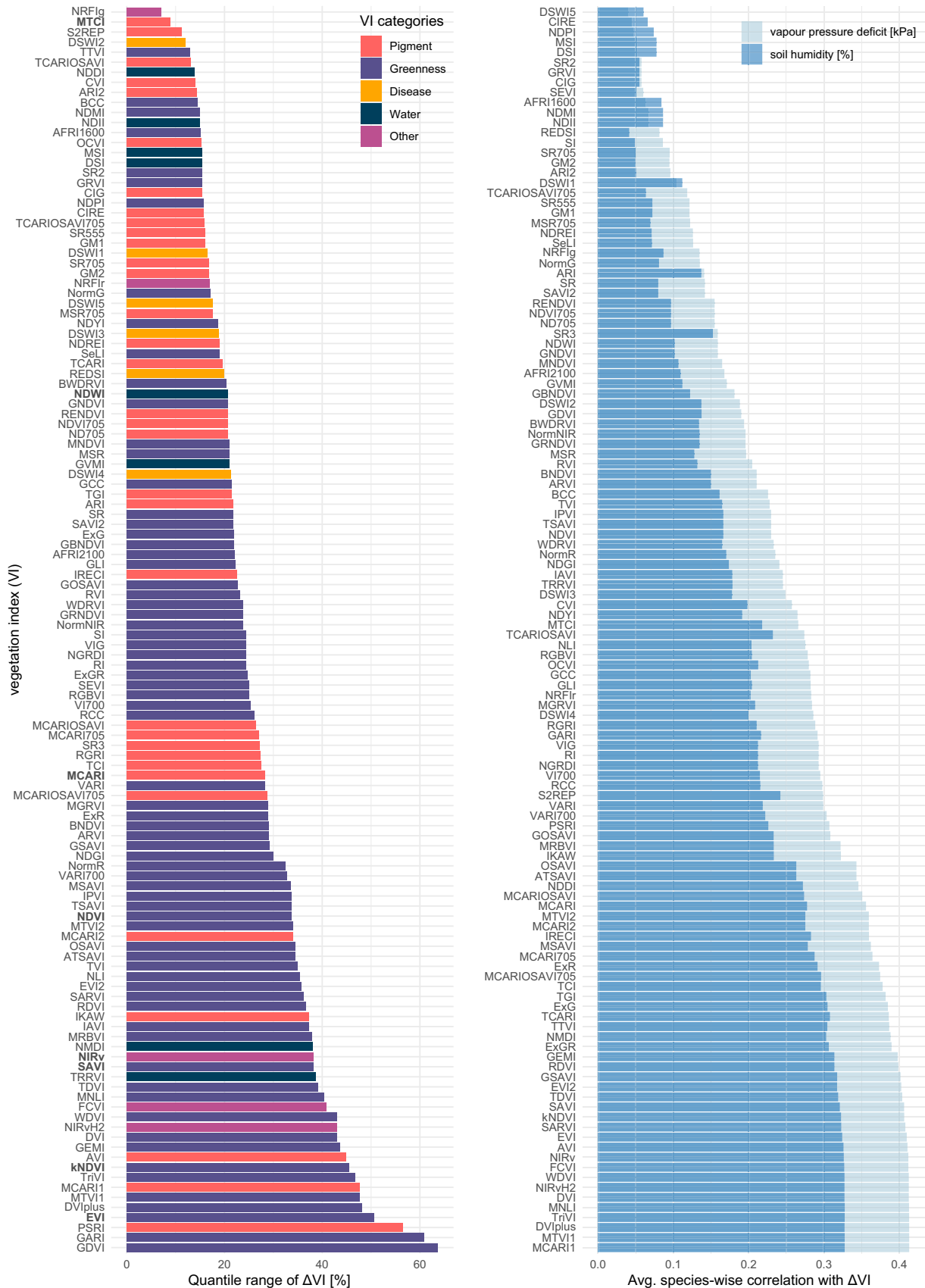


Fig. 5 | The effect (ΔVI) of vertical leaf angle dynamics on 124 vegetation indices. ΔVI % (left) is the relative difference of vegetation index values with and without integrating actual vertical leaf angle dynamics. The mean of the absolute correlation per species of ΔVI with relative soil moisture and vapor pressure deficit

(right) highlights that the effect of vertical leaf angles on VIs is controlled by environmental variables, which may not be related to the variable of interest (e.g. chlorophyll content). Indices shown in Fig. 4 are highlighted with bold font.

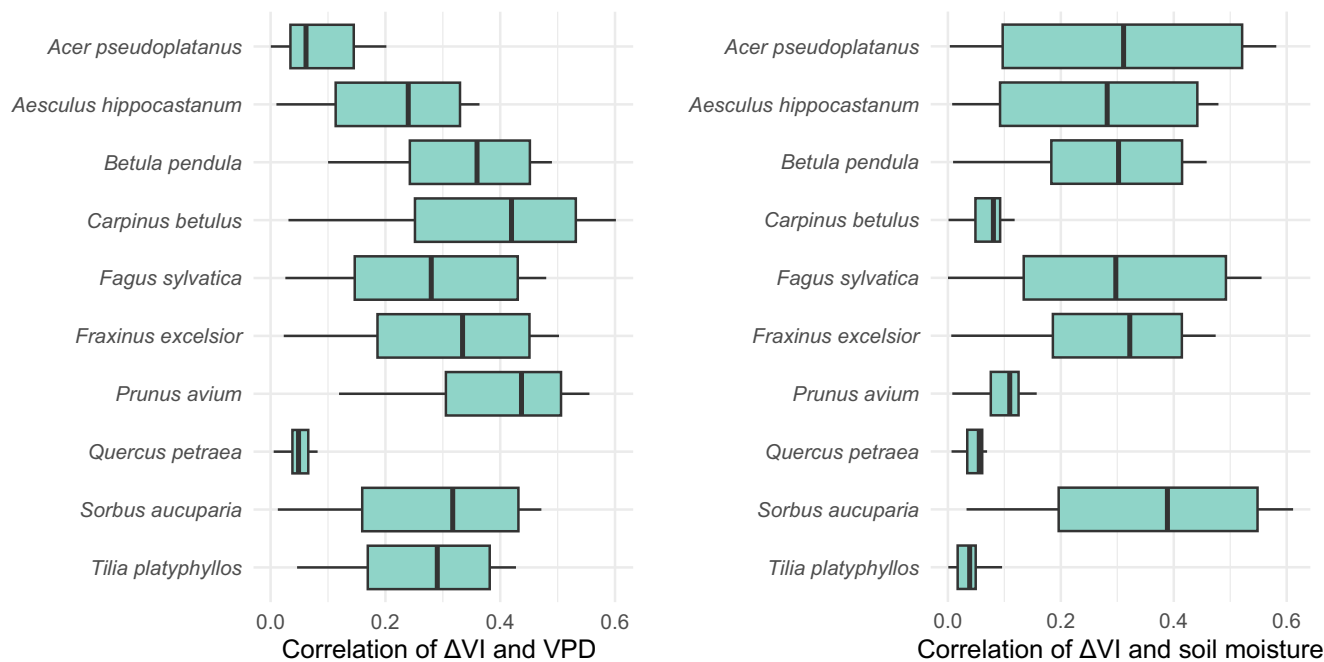


Fig. 6 | Species-wise absolute correlations of Δ VI across all 124 vegetation indices with environmental conditions. Correlations are measured using (Pearson's r) and derived for vapor pressure deficit (VPD, kPa, left) and soil moisture at 0.05 m depth

(%, right). The boxes show the interquartile range (IQR) and median, while the whiskers extend to the smallest and largest values within 1.5 times the IQR.

with LAD dynamics (Pearson's r) is significantly lower for VIs integrating a shortwave infrared band at 1610 nm ($p < 0.05$) and higher with the integration of the Red ($p < 0.05$) and Near-infrared bands ($p < 0.1$). There is a significant trend that LAD dynamics have a stronger impact on VIs of greater complexity (integrating more bands or arithmetic operations), both in terms of their value range (Δ VI%, $r = 0.26$, $p < 0.01$) and correlation with LAD dynamics ($r = 0.33$, $p < 0.01$). Details on the relationship of the VI configuration and LAD effects are given in Supplementary Fig. 4.

As indicated above, LAD dynamics are closely related to the above-described environmental dynamics, such as VPD and soil moisture. These environmentally controlled LAD dynamics are imprinted in the variation of vegetation indices (Fig. 5b, see also Supplementary Figs. 6 and 7 for air temperature and relative air humidity). Consequently, the temporal dynamics of vegetation indices, such as, a chlorophyll index, may not necessarily indicate changes in the biophysical or biochemical properties of interest, e.g., pigment contents, but might be confounded by the environmental conditions due to their imprint on leaf angles.

In the context of environmental conditions, it is important to note that the imprint of environmental variables on leaf angle dynamics differed between tree species (Supplementary Tab. 1–3). Species-wise correlations for vertical leaf angle dynamics and environmental variables (Pearson r) showed considerable variation, with r values ranging from -0.5 to 0.6 for soil moisture, from -0.19 to 0.64 for water pressure deficit, and from -0.18 to 0.63 for air temperature. Similarly, we find that only 10% of the LAD dynamics could be explained by linear models and recordings on temperature, soil moisture, and vapor pressure deficit, while mixed-effect models considering species as random effects explained 27% of the LAD variation. Thus, the species-specific response of LAD dynamics to environmental stimuli results in species-specific confounding effects of LAD dynamics on VIs (Fig. 6).

Discussion

By analyzing 124 commonly used VIs across 10 different plant species, we show that VIs can be substantially influenced by variations in vertical leaf angle dynamics, posing considerable challenges to their applicability and interpretation. The magnitude of this confounding effect varies by VI, differs

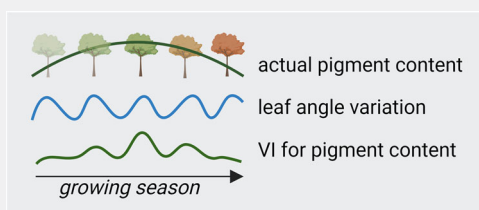
across species, and is driven by environmental dynamics. The impact on VI values varied between 7.93 and 59.54 % of their expected range. This implies that when considerable LAD dynamics are expected, some VIs should not be used for causal inference of those biochemical or structural plant properties for which they were initially designed or are frequently applied.

Previous studies have concluded that other factors, such as soil properties or the LAI, have a more substantial effect on VI variation than vertical leaf angle dynamics^{50–52}. However, the relative impact among these factors depends on the LAD variation considered, while previous studies did not evaluate real and continuous data on vertical leaf angle dynamics. Instead, previous findings were restricted to static or even heuristically defined species-specific LADs³⁴. Still, only a few studies could showcase the imprint of LAD dynamics for a few VIs (see, e.g., ref. 21), but only with small quantities of LAD observations. Using continuous and long-term measurements of LAD dynamics, we show that the effect of vertical leaf angle dynamics across 124 VI values is often not negligible. Ignoring LAD-VI dependencies may lead to incorrect conclusions about plant trait variation. We expect that this effect is particularly crucial at high temporal and spatial resolutions, such as Sentinel-2 or Landsat data, where individual pixels often correspond to individual crowns. At coarse spatial resolutions, such as with MODIS satellite data, we expect the imprint of vertical leaf angles to be reduced considerably due to mixed species or land cover types within a pixel.

We found that for most periods in time, VIs may only be moderately affected by vertical leaf angle dynamics (see data density in Fig. 4) as environmental conditions are stable or mild and, hence, do not exhibit a strong forcing of LAD dynamics (Supplementary Fig. 1). However, certain periods may show a strong variation in environmental conditions (e.g., peak VPD at climate extremes) or reach a critical level (e.g., soil moisture approaching the wilting point), which in turn induces a considerable variation in vertical leaf angles (Fig. 5b) with a large effect on most VIs (Δ VI% range, Fig. 5a). This is particularly critical for remote sensing applications-based ecosystem monitoring, e.g. tracking plant physiology during climate extremes or plant disease outbreaks (see Box 1), where high LAD dynamics are expected to covary with variables of interest, such as pigment or water contents,^{7,27}. In such situations, the LAD dynamics may bias or occlude the relationship between the VI values and the plant property of interest (Fig. 5).

Box 1 | Possible implications of VI-LAD dependency for remote sensing applications

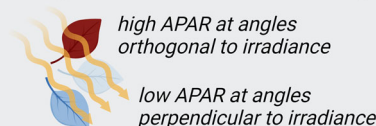
Monitoring vegetation greenness & vitality status: for monitoring ecosystems in the face of degradation, pests, pathogens, or climate extremes, VIs are a common method to approximate responses in the greenness, pigment, or water content of plant canopies⁴. However, as shown here, the temporal variation of related VI values can be severely confounded by LAD dynamics. Additionally, LAD dynamics themselves can be an immediate physiological response to environmental conditions^{7,27,37}. Thus, disentangling different plant morphological and physiological responses, such as variability in LAD, leaf biochemistry, or LAI, is vital for fully exploiting the potential of reflectance data^{7,27}. In this context, the presented comparisons of VIs across application domains (Fig. 5a) may provide a basis for selecting robust VIs for approximating different physiological and morphological plant properties. Still, the capacity of a VIs for indicating certain plant properties can be highly variable and should be thoroughly tested for the application case at hand⁴.



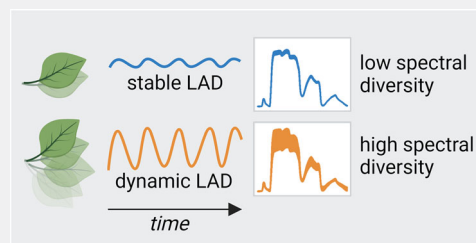
Tracking ecosystem functional & physiological properties: LAD dynamics can strongly confound VIs but these dynamics, resulting from environmental forcing and physiological responses, may also facilitate tracking ecosystem functional processes, such as primary productivity. For instance, vertical leaf angles control the absorbed photosynthetically active radiation (APAR) and can, thus, have a strong imprint on the productivity of plants⁶⁷. Here, indices with a strong sensitivity to NIR reflectance, including NIRv, kNDVI, and EVI^{30,46,68}, were shown to be most strongly confounded by LAD dynamics (Fig. 5). Together with information on solar radiance, these VIs were also shown to be valuable proxies to estimate gross primary productivity^{1,46,47}. Thus, the temporal dynamics of LADs and their effect on VIs may inherit information on the physiological status of plants. For instance, limited water availability during a drought may simultaneously lead to decreased productivity and hanging leaves,

which in turn alters canopy reflectance - particular in the NIR region⁶⁹. Thus, to some extent, the covariance of VIs with LAD dynamics may be both a challenge and an opportunity to monitor ecosystem properties and processes. More research is required for exploiting the links between plant movements, ecosystem functional processes, and Earth observation data.

Leaf angles control absorbed radiation, e.g. APAR:



Monitoring taxonomic & functional plant diversity: attempts to derive functional diversity from canopy reflectance typically assume a monotonic relationship of spectral variation with taxonomic or functional diversity^{10,70-72}. However, LAD dynamics may create spectral variation without a change in spectral or taxonomic plant diversity. Accordingly, plant species or communities with ample leaf angle dynamics (Fig. 6) may, hence, appear spectrally more diverse than canopies with few leaf angle dynamics - independent of the actual species richness or functional diversity. Thus, the LAD-related reflectance and VI dynamics through time may challenge both tracking the diversity of individual sites and comparing the diversity between sites (beta diversity). Such confounding effects on reflectance-based biodiversity assessments may be a particular challenge given that diversity-related spectral variation among plant communities is often subtle⁷³⁻⁷⁷.



A resulting and pressing question for future research is if such VI-based plant physiological assessments are then systematically over- or underestimated.

Such issues are further complicated given that LAD dynamics differ between species due to functional differences, such as leaf toughness or water-use strategy⁵³ and corresponding sensitivities to environmental drivers (Supplementary Tab. 1-3) and so does its imprint on VI values (Supplementary Fig. 5). Thus, a relationship between a VI and plant properties of interest (e.g., MCARI vs. pigments) may vary not only through time but also in space depending on the distribution of species or plant functional types and their specific leaf angle behavior.

Our results thus highlight that a naive interpretation of VIs can lead to wrong conclusions. A large share of VIs have been developed with reflectance data that was directly measured at individual leaves, where canopy structural variation was not considered in the index design (e.g., the photochemical reflectance index, PRI⁵⁴). Moreover, many indices developed at the canopy-level reflectance data were not explicitly created to be transferable across structural variation and not tested in this context^{4,55}. Generally, our findings stress that interpreting VI dynamics in a spatiotemporal setting should involve an a priori evaluation if the VI actually robustly indicates the variable of interest. For some target variables, indices may not

provide a robust indicator for a multitemporal or multi-species setting. In such cases, more complex methods that enable the compensation of structural reflectance features may be the right choice, e.g., the inversion of radiative transfer models^{7,27,43}, which can consider LAD dynamics or data-driven approaches that indirectly learn structural features from observations⁴⁴.

As indices are typically not designed in the context of LAD dynamics, our findings may provide a basis for choosing a robust index for monitoring vegetation properties over time, for instance, for tracking pigments, greenness, diseases, or water content (Fig. 5). We found a tendency that more simple indices were less affected by LAD dynamics. Moreover, we found that VIs incorporating red-edge bands had a lower ΔVI . This is particularly relevant for pigment indices, where VIs incorporating red-edge bands, such as MTCI or CVI, are more robust than indices that are limited to red and near-infrared bands, such as MCARI or PSRI (Fig. 4).

This is consistent with previous studies reporting that red-edge information is sensitive to structural leaf and canopy properties, and therefore incorporating red-edge bands can compensate for structural changes during the estimation of biochemical constituents or LAI⁵⁶⁻⁵⁹. This example of the red-edge index family indicates that indices can be designed to be less sensitive to LAD dynamics.

While our results are based on 10 temperate deciduous tree species, we expect similar effects for other functional types and biomes, such as angiosperms with softer leaves (less stable leaf structure). Clearly, not all plants may show pronounced leaf angle dynamics. Many gymnosperms, such as coniferous trees with very stable needles, are expected to show less variation in leaf angles. Yet, the movement of woody plant elements, such as branch or tree sway, may also change the canopy structure and thus reflectance patterns⁶⁰. Given that tree and branch movement strongly depends on environmental factors, such as wind and plant hydration status, both short- and long-term dynamics can be expected. Still, leaf and plant movements and their interaction with environmental drivers as well as other plant physiological responses remain an understudied phenomenon with substantial implications for remote sensing applications^{34,35}. Novel technologies, such as computer vision applications, robotics, phenocams, terrestrial laser scanning, or accelerometers^{37,61–64}, may help us to understand its implications for ecosystem monitoring with Earth observation data.

Our simulations did not account for correlations between leaf angle dynamics and other plant properties. First, we excluded correlations between vertical leaf angle dynamics and other biochemical and biophysical vegetation characteristics to isolate the specific effect of leaf angles. Second, these correlations are unknown or assumed to be relatively weak, variable across species, site, and environmental conditions, and difficult to obtain^{24,65}. Specifically, measuring plant properties, such as water content or chlorophyll content, at high temporal frequencies is extremely challenging and costly. Future studies could explore the coordination between leaf angles and other plant properties by incorporating extended observation periods.

Conclusions

Vegetation indices derived from reflectance signals acquired with Earth observation satellites provide a pivotal data stream to monitor Earth's terrestrial vegetation dynamics. However, temporal dynamics in vertical leaf angles can strongly alter reflectance signals and, hence, vegetation indices. We found that commonly used vegetation indices are systematically confounded by vertical leaf angle dynamics. For most indices, this effect scales monotonously with the magnitude of change in leaf angle distribution. We observed that such leaf angle dynamics are often strongly correlated with abiotic environmental variables. Such a change in VIs induced by environmental drivers may be spuriously interpreted as a change in the plant property for which the vegetation index was designed as an indicator - even if this property did not change at all. These systematic biases can limit the robustness of VIs for assessing plant properties in time series analysis and environmental monitoring. Therefore, interpreting the temporal patterns of VIs can result in wrong conclusions about plant and ecosystem processes. The anticipated rise in the frequency and severity of climate extremes could potentially lead to increased variability in the dynamic of vertical leaf angles and related confounding effects on vegetation indices. This is further complicated as leaf angle dynamics vary across species. Thus, spatial and temporal patterns found in VI products may not indeed indicate an actual variability of a plant property, but can be, among other factors, confounded by species-specific LAD and dynamics thereof. These findings indicate both challenges and opportunities for VI-based remote sensing. Some VIs may not be robust against variation in vertical leaf angles to monitor the spatiotemporal dynamics of plant properties for which they have been designed. At the same time, some spectral bands and indices (e.g., red-edge bands or the NIRv index) scale very tightly with changes in vertical leaf angles. Corresponding spectral mechanisms may facilitate the development of more robust indices against leaf angle variation or may open avenues to track processes related to leaf angle dynamics (e.g., ecosystem functional properties and fluxes thereof).

Methods

Retrieval of LAD dynamics

LADs were acquired using the computer vision method AngleCam³⁷, which is based on Convolutional Neural Networks applied on RGB photos.

Temporal dynamics of leaf angles can be derived by applying AngleCam to photo time series derived from time-lapse cameras. For this, we used the Brinno TLC200-Pro (Brinno Europe, The Netherlands), which acquires RGB photos with a resolution of 1280 × 720. Note, that also other, similar camera models are compatible with AngleCam, as the method was trained with a variety of camera models. AngleCam predicts LADs from such photos in 2-degree intervals from 0 to 90°, where 0 corresponds to a horizontal leaf surface angle and 90 to a vertical leaf surface angle (Fig. 3).

We predicted LADs with AngleCam from photo time series acquired across 10 tree species in the MyDiv tree experiment (Mycorrhiza in tree Diversity effects on ecosystem functioning). The MyDiv experiment is located in Germany, at the Bad Lauchstädt Experimental Research Station of the Helmholtz Centre for Environmental Research-UFZ (51°23' N, 11°53' E). MyDiv comprises 80 plots with a systematic design of tree species, including monocultures and polycultures of 2 or 4 tree species. For this study, we only assessed vertical leaf angle variation in monoculture plots. The species include *Acer pseudoplatanus* L., *Aesculus hippocastanum* L., *Fraxinus excelsior* L., *Prunus avium* (L.)L., *Sorbus aucuparia* L., *Betula pendula* Roth, *Carpinus betulus* L., *Fagus sylvatica* L., *Quercus petraea* (Matt.) Liebl., *Tilia platyphyllos* Scop. Respective tree individuals were regularly planted in 11 m by 11 m grids with 1 m spacing. A detailed description of the MyDiv experimental site can be found in ref. 40. During sampling, the tree species were nine years old, and top canopy heights ranged from approximately 3.3 to 7.3 m.

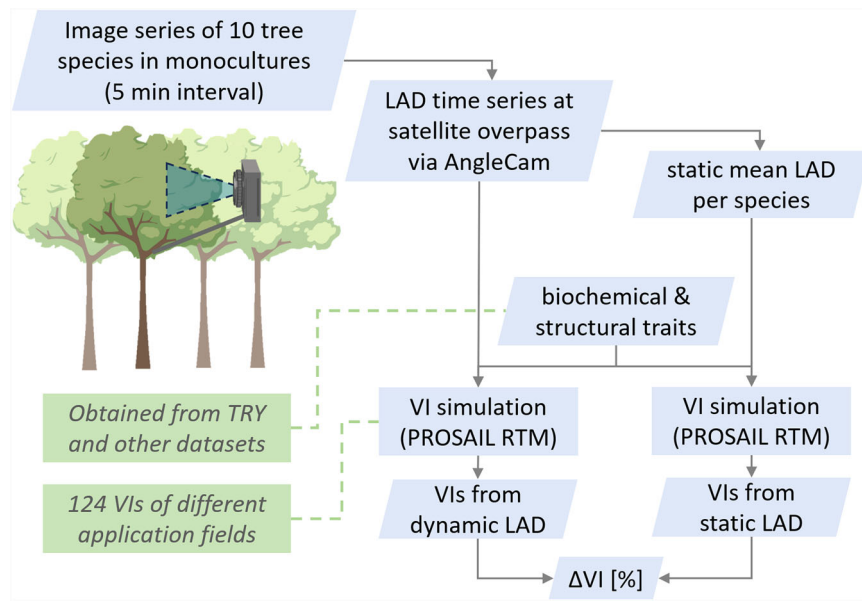
For each species, we placed two time-lapse cameras in one monoculture plot. The image time series was acquired within the significant part of the vegetation period from June 6th to October 5th, 2022. The cameras had a horizontal field of view, capturing branches of two tree individuals located in the central area of the plot with a distance of 40–80 cm (Fig. 7). The two cameras were affixed to an aluminum pole, orthogonally attached to one of the trees near the central area of the plot. The mounting height corresponded to the upper third of the tree crowns. The cameras were configured to capture images at 5-minute intervals in High Dynamic Range (HDR) mode. Maintenance occurred roughly every four weeks, involving tasks such as battery replacement, checking the camera orientation, removal of dust and pollen from the lenses, and the transfer of captured imagery.

We re-trained the AngleCam models to ensure that the method is transferable to the conditions at the MyDiv site and its tree species. For this, we sampled 1000 images from the above-described time-lapse imagery. We generated LAD labels for each of these sampled images, using the visual interpretation procedure described and evaluated in ref. 37. The new sample data was added to the training data described in³⁷ to retrain the AngleCam model (the updated version of AngleCam is available at: <https://github.com/tejakattenborn/AngleCAM>).

We applied the retrained AngleCam model to all available time-lapse photos falling within the overpass times around solar noon (10:00 - to 11:00) of typical optical Earth observation satellite missions, such as Sentinel-2, Landsat, MODIS Terra (Fig. 3). The LADs obtained from AngleCam for these time periods were averaged, resulting in an average LAD at solar noon per camera and day (Supplementary Fig. 2). Through the averaging in this time period, uncertainties of individual LAD retrievals, e.g. resulting from wind or illumination effects, were effectively reduced.

Satellite reflectance and VI simulation. For each daily LAD, vegetation indices were simulated using the radiative transfer model (RTM) PROSAIL (Fig. 7). PROSAIL is a process-based RTM that can simulate the reflectance of vegetation canopies from 400–2500 nm with 1 nm spectral resolution³⁸. PROSAIL combines the PROSPECT model, which simulates the optical properties of leaves (in this case, PROSPECT-D¹⁸), with the 4SAIL2 model³⁸, which simulates canopy-scale reflectance based on vegetation structural properties and the sun-observer geometry. Typically, LADs in PROSAIL are parametrized using an average vertical leaf angle or a two-factor parameter distribution function⁴³. Here, we modified the LAD input dimension of PROSAIL to 2-degree intervals (43

Fig. 7 | Workflow from leaf angle distributions retrieval and subsequent vegetation indices simulation. For each species, the effect of leaf angle distributions (LAD) on vegetation indices (VI) was determined as the relative difference of VIs derived from actual LAD dynamics and average LADs.



instead of 13 bins), enabling direct compatibility with the AngleCam-derived LADs.

In addition to the observed LAD, we further varied the vegetation properties implemented in PROSAIL to simulate a representative variation of the reflectance and VI ranges for each tree species (Fig. 7). These other biochemical and biophysical vegetation properties were randomly sampled to isolate the specific imprint of leaf angles on vegetation indices. The values for these vegetation properties were sampled from a uniform distribution within the following ranges: LAI 1–5 m²/m², leaf chlorophyll content 27–68 μg/cm², leaf carotenoid content 3.8–9.7 μg/cm², leaf anthocyanin content 0.57–1.44 μg/cm², leaf water content 0.008–0.026 mg/cm², and leaf mass per area 0.003–0.011 mg/cm². These value ranges were based on a merged dataset composed of a database curated by Cherif et al. 2023⁴⁴ and the TRY database⁴⁵ (vers. 5). Furthermore, these datasets were used to derive empirical correlations among vegetation properties within the above-described ranges. Leaf carotenoid content was calculated by dividing leaf chlorophyll by 7 and adding normally distributed noise (SD = 1.1), while leaf anthocyanin content was calculated by dividing leaf chlorophyll content by 47 with normally distributed noise added (SD = 0.55). Leaf equivalent water thickness was derived from LMA multiplied by 2.4, with normally distributed noise (SD = 0.0023) included.

The simulated 1 nm reflectance spectra derived from PROSAIL were converted to multispectral reflectance at Sentinel-2A bands using established spectral response functions (see <https://github.com/jbferet/prosail>). These multispectral reflectances of these Sentinel-2A bands were used to calculate index values for 124 common VIs using the Python package *spyndex* (v0.3)⁶. For indices that require additional parameters, the latter were set to values as reported in their primary studies (e.g. σ for kNDVI).

The impact of LAD dynamics on VI values (onward ΔVI) was determined as the difference of (i) VI values simulated from daily LAD dynamics of a given camera and (ii) VI values simulated from a static mean LAD of the entire period of the same camera (Eq. (1)). To facilitate the comparison of LAD sensitivities of the different VIs, ΔVI values were normalized to relative values (%) using the obtained value range of the respective index (0.01–0.99 quantiles). These ranges were derived from indices without considering LAD dynamics.

$$\Delta VI\% = \frac{\frac{1}{n} \sum_{i=1}^n VI_{\text{staticLAD}_i} - VI_{\text{dynamicLAD}_i}}{Q_{99}(VI_{\text{staticLAD}}) - Q_{01}(VI_{\text{staticLAD}})} \quad (1)$$

Characterization of indices by application and complexity. To ease the interpretation of ΔVI of the different VIs, we grouped all VIs according to common application domains, including:

- Greenness, representing VIs designed to estimate LAI, vegetation density, or foliage and above-ground biomass (e.g. the Normalized Difference Vegetation Index, NDVI),
- Pigments, representing VIs for Chlorophyll, Carotenoid, vegetation health, and greenness (e.g. Red-Edge Chlorophyll Index, $CI_{\text{red-edge}}$),
- Water, representing VIs designed to track leaf water status, such as Normalized Difference Water Index (NDWI) or Disease Water Stress Index (DSWI1),
- Disease, representing VIs for tracking vegetation health, pests, and pathogens, e.g. Red-Edge Disease Stress Index (REDSI),
- Other, VIs that do not fit into the above-mentioned categories (e.g. Near-Infrared Reflectance of Vegetation Index, NIRv).

Note, that these groupings were chosen heuristically, while indices may be used for different applications.

Moreover, we compared $\Delta VI\%$ values with respect to the complexity of VIs, that is how many bands or arithmetic operations are used in the formulation of an index.

Relating LAD and VI dynamics with environmental drivers. We assessed the correlation of LAD and their effect on VI dynamics (ΔVI) within the context of environmental variables. The correlation and their significance were quantified across all species and separately for each species using Pearson’s correlation coefficient (r). A time series of environmental variables were recorded using three climate stations in three plots of the MyDiv site at 1 m height. The climate stations are based on a customized setup described in ref. 66. Air humidity [%] and air temperature [°C] were tracked with a SHT21 sensor (Sensirion, Germany). Soil moisture [%] at 5, 10, and 55 cm depth was measured with a SMT100 sensor (Truebner GmbH, Germany). After initial testing, we focussed on the soil moisture dynamics at 5 cm depth since it showed the most variability, e.g., in response to precipitation events. Based on these measurements, we also derived the vapor pressure deficit (VPD) [kPa] using Eq. (3):

$$VPD = \left(1 - \frac{RH}{100}\right) \times \frac{e_s}{1000} \quad (2)$$

where RH is the relative humidity and e_s is the saturation vapor pressure in millibars. e_s can be approximated by the Tatens equation (3):

$$e_s = 610.78 \times \exp\left(\frac{T}{T + 237.3} \times 17.2694\right) \quad (3)$$

here, T is the ambient air temperature in °C.

Reporting summary

Further information on research design is available in the Nature Portfolio Reporting Summary linked to this article.

Code availability

The AngleCam method (computer vision-based estimation of vertical leaf angles) is openly available at <https://github.com/tejakattenborn/AngleCAM>. All other code for reproducing the results, including the code for simulating reflectance spectra, calculating the 124 vegetation indices and the statistical analytics are available at: <https://doi.org/10.5281/zenodo.12775222>.

Data availability

The data used for this study are available at <https://doi.org/10.5281/zenodo.12775222>. This includes the observed leaf angle distributions (derived from the AngleCam method) and the environmental data. Part of the trait data of this study comes from the TRY database (and can be requested from <https://www.try-db.org/>) or from⁴⁴ and is available from the corresponding repository: <https://gitlab.com/eya95/multi-traitretrieval>.

Received: 13 April 2024; Accepted: 20 September 2024;

Published online: 02 October 2024

References

- Zeng, Y. et al. Optical vegetation indices for monitoring terrestrial ecosystems globally. *Nat. Rev. Earth Environ.* **3**, 477–493 (2022).
- Homolová, L., Malenovsky, Z., Clevers, J. G., Garcia-Santos, G. & Schaepman, M. E. Review of optical-based remote sensing for plant trait mapping. *Ecol. Complex.* **15**, 1–16 (2013).
- Wang, Z. et al. Mapping foliar functional traits and their uncertainties across three years in a grassland experiment. *Remote Sens. Environ.* **221**, 405–416 (2019).
- Xue, J. & Su, B. Significant remote sensing vegetation indices: a review of developments and applications. *J. Sens.* **2017**, 1353691 (2017).
- Tucker, C. J. Red and photographic infrared linear combinations for monitoring vegetation. *Remote Sens. Environ.* **8**, 127–150 (1979).
- Montero, D. et al. A standardized catalogue of spectral indices to advance the use of remote sensing in earth system research. *Sci. Data* **10**, 197 (2023).
- Zarco-Tejada, P. J. et al. Previsual symptoms of xylella fastidiosa infection revealed in spectral plant-trait alterations. *Nat. Plants* **4**, 432–439 (2018).
- Piao, S. et al. Characteristics, drivers and feedbacks of global greening. *Nat. Rev. Earth Environ.* **1**, 1–14 (2019).
- Cortés, J. et al. Where are global vegetation greening and browning trends significant? *Geophys. Res. Lett.* **48**, e2020GL091496 (2021).
- Ma, X. et al. Inferring plant functional diversity from space: the potential of sentinel-2. *Remote Sens. Environ.* **233**, 111368 (2019).
- North, P. R. Estimation of fapar, lai, and vegetation fractional cover from atsr-2 imagery. *Remote Sens. Environ.* **80**, 114–121 (2002).
- Silleos, N. G., Alexandridis, T. K., Gitas, I. Z. & Perakis, K. Vegetation indices: advances made in biomass estimation and vegetation monitoring in the last 30 years. *Geocarto Int.* **21**, 21–28 (2006).
- Mahecha, M. D., Fürst, L. M., Gobron, N. & Lange, H. Identifying multiple spatiotemporal patterns: A refined view on terrestrial photosynthetic activity. *Pattern Recognit. Lett.* **31**, 2309–2317 (2010).
- Estupinan-Suarez, L. M. et al. Spatial patterns of vegetation activity related to enso in northern south america. *J. Geophys. Res. Biogeosci.* **129**, e2022JG007344 (2024).
- Claverie, M. et al. The harmonized landsat and sentinel-2 surface reflectance data set. *Remote Sens. Environ.* **219**, 145–161 (2018).
- Ganguly, S., Friedl, M. A., Tan, B., Zhang, X. & Verma, M. Land surface phenology from modis: characterization of the collection 5 global land cover dynamics product. *Remote Sens. Environ.* **114**, 1805–1816 (2010).
- Kokaly, R. F., Asner, G. P., Ollinger, S. V., Martin, M. E. & Wessman, C. A. Characterizing canopy biochemistry from imaging spectroscopy and its application to ecosystem studies. *Remote Sens. Environ.* **113**, S78–S91 (2009).
- Féret, J.-B., Gitelson, A., Noble, S. & Jacquemoud, S. Prospect-d: towards modeling leaf optical properties through a complete lifecycle. *Remote Sens. Environ.* **193**, 204–215 (2017).
- Kattenborn, T., Fassnacht, F. E. & Schmidtlein, S. Differentiating plant functional types using reflectance: which traits make the difference? *Remote Sens. Ecol. Conserv.* **5**, 5–19 (2019).
- Zeng, Y. et al. Structural complexity biases vegetation greenness measures. *Nat. Ecol. Evol.* **7**, 1790–1798 (2023).
- Hase, N. et al. Identifying the main drivers of the seasonal decline of near-infrared reflectance of a temperate deciduous forest. *Agric. For. Meteorol.* **313**, 108746 (2022).
- Wu, G. et al. Difference in seasonal peak timing of soybean far-red sif and gpp explained by canopy structure and chlorophyll content. *Remote Sens. Environ.* **279**, 113104 (2022).
- Darwin, C. & Darwin, F. *The Power Of Movement In Plants* (John Murray, 1880).
- Van Zanten, M., Pons, T., Janssen, J., Voeselek, L. & Peeters, A. On the relevance and control of leaf angle. *Crit. Rev. Plant Sci.* **29**, 300–316 (2010).
- Xu, F., Guo, W., Xu, W., Wei, Y. & Wang, R. Leaf morphology correlates with water and light availability: what consequences for simple and compound leaves? *Prog. Nat. Sci.* **19**, 1789–1798 (2009).
- Ross, I. *The Radiation Regime And Architecture Of Plant Stands* (Springer Science & Business Media, 1981).
- Zarco-Tejada, P. J. et al. Divergent abiotic spectral pathways unravel pathogen stress signals across species. *Nat. Commun.* **12**, 6088 (2021).
- Jackson, R. D. & Pinter Jr, P. J. Spectral response of architecturally different wheat canopies. *Remote Sens. Environ.* **20**, 43–56 (1986).
- Zou, X., Zhu, S. & Möttus, M. Estimation of canopy structure of field crops using sentinel-2 bands with vegetation indices and machine learning algorithms. *Remote Sens.* **14**, 2849 (2022).
- Zeng, Y. et al. A practical approach for estimating the escape ratio of near-infrared solar-induced chlorophyll fluorescence. *Remote Sens. Environ.* **232**, 111209 (2019).
- Baret, F. & Guyot, G. Potentials and limits of vegetation indices for lai and apar assessment. *Remote Sens. Environ.* **35**, 161–173 (1991).
- Zou, X. et al. Effects of crop leaf angle on lai-sensitive narrow-band vegetation indices derived from imaging spectroscopy. *Appl. Sci.* **8**, 1435 (2018).
- McNeil, B. E. et al. Tree crown economics. *Front. Ecol. Environ.* **21**, 40–48 (2023).
- Ollinger, S. V. Sources of variability in canopy reflectance and the convergent properties of plants. *N. Phytol.* **189**, 375–394 (2011).
- Berger, K. et al. Crop nitrogen monitoring: recent progress and principal developments in the context of imaging spectroscopy missions. *Remote Sens. Environ.* **242**, 111758 (2020).
- Yang, X. et al. Leaf angle as a leaf and canopy trait: rejuvenating its role in ecology with new technology. *Ecol. Lett.* **26**, 1005–1020 (2023).
- Kattenborn, T., Richter, R., Guimarães-Steinicke, C., Feilhauer, H. & Wirth, C. Anglecam: predicting the temporal variation of leaf angle

- distributions from image series with deep learning. *Methods Ecol. Evolution* **13**, 2531–2545 (2022).
38. Verhoef, W. & Bach, H. Coupled soil–leaf–canopy and atmosphere radiative transfer modeling to simulate hyperspectral multi-angular surface reflectance and toa radiance data. *Remote Sens. Environ.* **109**, 166–182 (2007).
 39. Sodoge, J., Kuhlicke, C., Mahecha, M. D. & de Brito, M. M. Text mining uncovers the unique dynamics of socio-economic impacts of the 2018–2022 multi-year drought in Germany. *Nat. Hazards Earth Syst. Sci.* **24**, 1757–1777 (2024).
 40. Ferlian, O. et al. Mycorrhiza in tree diversity–ecosystem function relationships: conceptual framework and experimental implementation. *Ecosphere* **9**, e02226 (2018).
 41. Schumacher, D. L. et al. Detecting the human fingerprint in the summer 2022 west-central European soil drought. *EGUosphere* **2023**, 1–41 (2023).
 42. Altermann, M. et al. Chernozem—soil of the year 2005. *J. Plant Nutr. Soil Sci.* **168**, 725–740 (2005).
 43. Jacquemoud, S. et al. Prospect+ soil models: a review of use for vegetation characterization. *Remote Sens. Environ.* **113**, S56–S66 (2009).
 44. Cherif, E. et al. From spectra to plant functional traits: Transferable multi-trait models from heterogeneous and sparse data. *Remote Sens. Environ.* **292**, 113580 (2023).
 45. Kattge, J. et al. Try plant trait database—enhanced coverage and open access. *Glob. Change Biol.* **26**, 119–188 (2020).
 46. Camps-Valls, G. et al. A unified vegetation index for quantifying the terrestrial biosphere. *Sci. Adv.* **7**, eabc7447 (2021).
 47. Badgley, G., Field, C. B. & Berry, J. A. Canopy near-infrared reflectance and terrestrial photosynthesis. *Sci. Adv.* **3**, e1602244 (2017).
 48. Huete, A. A soil-adjusted vegetation index (savi). *Remote Sens. Environ.* **25**, 295–309 (1988).
 49. Huete, A. et al. Overview of the radiometric and biophysical performance of the modis vegetation indices. *Remote Sens. Environ.* **83**, 195–213 (2002).
 50. Rondeaux, G., Steven, M. & Baret, F. Optimization of soil-adjusted vegetation indices. *Remote Sens. Environ.* **55**, 95–107 (1996).
 51. Steven, M. D. The sensitivity of the osavi vegetation index to observational parameters. *Remote Sens. Environ.* **63**, 49–60 (1998).
 52. Goward, S. N. & Huemmrich, K. F. Vegetation canopy par absorptance and the normalized difference vegetation index: an assessment using the sail model. *Remote Sens. Environ.* **39**, 119–140 (1992).
 53. Hartmann, H., Link, R. M. & Schuldt, B. A whole-plant perspective of isohydry: stem-level support for leaf-level plant water regulation. *Tree Physiol.* **41**, 901–905 (2021).
 54. Peñuelas, J., Filella, I. & Gamon, J. A. Assessment of photosynthetic radiation-use efficiency with spectral reflectance. *N. Phytol.* **131**, 291–296 (1995).
 55. Bannari, A., Morin, D., Bonn, F. & Huete, A. A review of vegetation indices. *Remote Sens. Rev.* **13**, 95–120 (1995).
 56. Horler, D., Dockray, M. & Barber, J. The red edge of plant leaf reflectance. *Int. J. Remote Sens.* **4**, 273–288 (1983).
 57. Dong, T. et al. Assessment of red-edge vegetation indices for crop leaf area index estimation. *Remote Sens. Environ.* **222**, 133–143 (2019).
 58. Sims, D. A. & Gamon, J. A. Relationships between leaf pigment content and spectral reflectance across a wide range of species, leaf structures and developmental stages. *Remote Sens. Environ.* **81**, 337–354 (2002).
 59. Zarco-Tejada, P. J. et al. Chlorophyll content estimation in an open-canopy conifer forest with sentinel-2a and hyperspectral imagery in the context of forest decline. *Remote Sens. Environ.* **223**, 320–335 (2019).
 60. Jackson, T. et al. An architectural understanding of natural sway frequencies in trees. *J. R. Soc. Interface* **16**, 20190116 (2019).
 61. Jaeger, D. M. et al. From flowering to foliage: accelerometers track tree sway to provide high-resolution insights into tree phenology. *Agric. For. Meteorol.* **318**, 108900 (2022).
 62. Van Emmerik, T. et al. Measuring tree properties and responses using low-cost accelerometers. *Sensors* **17**, 1098 (2017).
 63. Junttila, S. et al. Tree water status affects tree branch position. *Forests* **13**, 728 (2022).
 64. Xiang, L. et al. Field-based robotic leaf angle detection and characterization of maize plants using stereo vision and deep convolutional neural networks. *J. Field Robot.* **40**, 1034–1053 (2023).
 65. Falster, D. S. & Westoby, M. Leaf size and angle vary widely across species: what consequences for light interception? *N. Phytol.* **158**, 509–525 (2003).
 66. Schädler, M. et al. Investigating the consequences of climate change under different land-use regimes: a novel experimental infrastructure. *Ecosphere* **10**, e02635 (2019).
 67. Fensholt, R., Sandholt, I. & Rasmussen, M. S. Evaluation of modis lai, fapar and the relation between fapar and ndvi in a semi-arid environment using in situ measurements. *Remote Sens. Environ.* **91**, 490–507 (2004).
 68. Dechant, B. et al. Canopy structure explains the relationship between photosynthesis and sun-induced chlorophyll fluorescence in crops. *Remote Sens. Environ.* **241**, 111733 (2020).
 69. Hwang, Y., Kim, J. & Ryu, Y. Canopy structural changes explain reductions in canopy-level solar induced chlorophyll fluorescence in prunus yedoensis seedlings under a drought stress condition. *Remote Sens. Environ.* **296**, 113733 (2023).
 70. Schneider, F. D. et al. Mapping functional diversity from remotely sensed morphological and physiological forest traits. *Nat. Commun.* **8**, 1441 (2017).
 71. Rocchini, D. et al. Remotely sensed spatial heterogeneity as an exploratory tool for taxonomic and functional diversity study. *Ecol. Indic.* **85**, 983–990 (2018).
 72. Pacheco-Labrador, J. et al. A generalizable normalization for assessing plant functional diversity metrics across scales from remote sensing. *Methods Ecol. Evol.* **14**, 2123–2136 (2023).
 73. Fassnacht, F. E., Müllerová, J., Conti, L., Malavasi, M. & Schmidlein, S. About the link between biodiversity and spectral variation. *Appl. Vegetation Sci.* **25**, e12643 (2022).
 74. Dronova, I. & Taddeo, S. Remote sensing of phenology: Towards the comprehensive indicators of plant community dynamics from species to regional scales. *J. Ecol.* **110**, 1460–1484 (2022).
 75. Nelson, P. R. et al. Remote sensing of tundra ecosystems using high spectral resolution reflectance: opportunities and challenges. *J. Geophys. Res. Biogeosci.* **127**, e2021JG006697 (2022).
 76. Schmidlein, S. & Fassnacht, F. E. The spectral variability hypothesis does not hold across landscapes. *Remote Sens. Environ.* **192**, 114–125 (2017).
 77. Ludwig, A., Doktor, D. & Feilhauer, H. Is spectral pixel-to-pixel variation a reliable indicator of grassland biodiversity? a systematic assessment of the spectral variation hypothesis using spatial simulation experiments. *Remote Sens. Environ.* **302**, 113988 (2024).

Acknowledgements

T.K. was partially funded by the Flexible Funds Program for junior scientists of the University of Leipzig (project number 232201582). T.K. received further funding from the German Research Foundation (DFG) under the projects *BigPlantSens* (project number 444524904), *PANOPS* (project number 504978936), and *ECOSENSE* (project number SFB 1537/1). N.E., O.F., T.K., C.W., C.G.S., L.S., H.F., M.H., M.D.M., and B.D. gratefully acknowledge the support of iDiv funded by the German Research Foundation (DFG- FZT 118, 202548816). B.D. was supported by sDiv, the

Synthesis Centre of iDiv. N.E. and O.F. acknowledge support by the DFG (Ei 862/29-1). L.S. was supported by the international research training Group TreeDi (GRK2324) jointly funded by the Deutsche Forschungsgemeinschaft (DFG, German Research Foundation) - 319936945 and the University of Chinese Academy of Science (UCAS).

Author contributions

T.K., S.W., and B.D. conceived the ideas and designed the methodology. O.F. and N.E. conceptualized, set up, and maintained the MyDiv experimental site. T.K. planned the data acquisition. C.G.S. and L.S. assisted in the sensor installation and maintenance. T.K., C.W., and R.R. developed AngleCam. T.K. applied AngleCam on the MyDiv data and performed the reflectance simulations. D.M. implemented the procedures for the VI calculation. T.K. performed the statistical analysis. T.K., S.W., D.M., M.D.M., R.R., C.G.S., C.W., O.F., H.F., L.S., N.E., and B.D. contributed critically to the drafts and gave final approval for publication.

Funding

Open Access funding enabled and organized by Projekt DEAL.

Competing interests

The authors declare no competing interests.

Additional information

Supplementary information The online version contains supplementary material available at <https://doi.org/10.1038/s43247-024-01712-0>.

Correspondence and requests for materials should be addressed to Teja Kattenborn.

Peer review information *Communications Earth & Environment* thanks the anonymous reviewers for their contribution to the peer review of this work. Primary Handling Editors: Joe Aslin, Mengjie Wang. A peer review file is available.

Reprints and permissions information is available at <http://www.nature.com/reprints>

Publisher's note Springer Nature remains neutral with regard to jurisdictional claims in published maps and institutional affiliations.

Open Access This article is licensed under a Creative Commons Attribution 4.0 International License, which permits use, sharing, adaptation, distribution and reproduction in any medium or format, as long as you give appropriate credit to the original author(s) and the source, provide a link to the Creative Commons licence, and indicate if changes were made. The images or other third party material in this article are included in the article's Creative Commons licence, unless indicated otherwise in a credit line to the material. If material is not included in the article's Creative Commons licence and your intended use is not permitted by statutory regulation or exceeds the permitted use, you will need to obtain permission directly from the copyright holder. To view a copy of this licence, visit <http://creativecommons.org/licenses/by/4.0/>.

© The Author(s) 2024